Materials Transactions, Vol. 49, No. 9 (2008) pp. 1953 to 1956

Three-Dimensional Observation of Dislocations by Electron Tomography in a Silicon Crystal

Masaki Tanaka[1], Masaki Honda[1,*], Masatoshi Mitsuhara[2], Satoshi Hata[2], Kenji Kaneko[1,3] and Kenji Higashida[1]

[1]*Department of Materials Science and Engineering, Kyushu University, Fukuoka 819-0395, Japan*
[2]*Department of Engineering Sciences for Electronics and Materials, Kyushu University, Kasuga 816-8580, Japan*
[3]*JST-CREST, Fukuoka 819-0395, Japan*

Dislocations in a silicon single crystal introduced by three point-bending at a high temperature were observed by electron tomography in annular dark field-scanning transmission electron microscopy (ADF-STEM). Commercially available P type (001) single crystal wafers were employed. An ADF STEM tilt series was acquired from -60° to $+60^\circ$ in tilt range with 2° in tilt step. The diffraction vector was maintained close to $\boldsymbol{g}(hkl) = 220$ during the acquisition by adjusting the [110] direction of the sample parallel to the tilt axis of the holder. The observed dislocations were reconstructed by simultaneous interactive reconstruction technique, exhibiting a 3-D configuration of dislocations introduced by the three-point bending. [doi:10.2320/matertrans.MAW200828]

(Received April 23, 2008; Accepted June 13, 2008; Published August 25, 2008)

Keywords: *mechanical property, scanning transmission electron microscopy (STEM), annular dark field (ADF)*

1. Introduction

Analyzing deformation microstructures is one of the key issues to understand the mechanical properties of crystalline materials. Particularly, dislocation configurations in plastically deformed materials are essential to various phenomena such as work-hardening. Quite a few direct observations of dislocations by electron microscopy have been carried out by many researchers since Hirsch *et al.*[1)] firstly observe dislocations in aluminum in 1956. It is still difficult, however, to clarify the thee-dimensional aspect of dislocations complexly tangled. Recently, electron tomography[2)] draws many interests to unveil the three-dimensional aspect of polymers, and many researchers have started to apply the method into the observations of particles in metallic materials.[3–6)] Barnard *et al.*[7,8)] proposed a new method of electron tomography using a week beam method to observe dislocations in a heteroepitaxial gallium nitride film and reconstruct to show that the dislocations penetrate the thin film.

The electron tomography observation of dislocations in deformed materials using BF and DF (weak-beam) showed some difficulties to obtain sharp images of dislocations throughout a tilting series of tomography since the image contrasts in those methods strongly depend on the diffraction conditions. A residual strain makes it difficult to obtain uniform background contrasts, which reduces the image quality. Annular dark-field scanning transmission electron microscopy (ADF-STEM) is less sensitive to the diffraction constant due to the convergent-beam, which allows large error from the exact Bragg condition to show dislocation images in the acquisition of the tilting series.

In the present study, we attempted to observe dislocations in slip bands formed in a silicon single crystal by electron tomography in ADF-STEM in order to demonstrate its potentialities to analyze three-dimensional configurations of dislocations.

*Graduate Student, Kyushu University

2. Experimental

Commercially available P type (001) single crystal wafers with the width of 0.65 mm were employed. The sample was cut to a 37×3.5 mm piece from the wafer. In order to increase the number of dislocation sources, a scratch was introduced at the middle of the plate along the $[1\bar{1}0]$ direction as shown in Fig. 1(a). In order to introduce dislocations, the sample was three-point bended at 1023 K with a cross head speed of 0.2 mm/min. The specimen geometry is shown in Fig. 1(a). The sample was kept deformed over yielding. The cross head was stopped when the maximum resolved shear stress reached 30 MPa. Figure 1(b) indicates an optical micrograph obtained from the bended sample around the scratch, showing slip bands parallel to the [110] directions. The area with the slip bands was thinned by ion milling (Fischione-1010). An ADF-STEM tilt series was acquired from -60° to $+60^\circ$ in tilt range with 2° in tilt step. The defocus of the images was adjusted by automatically/manually at every 2 step (4°) in the tilting series during the acquisition of the image. The diffraction vector was maintained close to $\boldsymbol{g}(hkl) = 220$ during the acquisition by adjusting the [110] direction of the sample parallel to the tilt axis of the holder, so that 220 diffraction disc was maintained to be within the annular detector during the acquisition of the STEM images. The inner angle of the detector was set at 45 mrad. ADF-STEM images of dislocations are nearly the same with those from conventional dark-field TEM, *i.e.*, diffraction contrasts are dominant to exhibit dislocation images. A specially designed high-angle triple-axis sample holder (HATA holder, Mel-Build, Japan) was used to minimize misorientations of the tilt axis from the [110] direction. ADF-STEM observation was performed using FEI TECNAI-F20 operating at 200 kV at Research Laboratory for High Voltage Electron Microscopy, Kyushu University. The observed dislocations were reconstructed by simultaneous interactive reconstruction technique (SIRT)[9)] with 20 cycles.

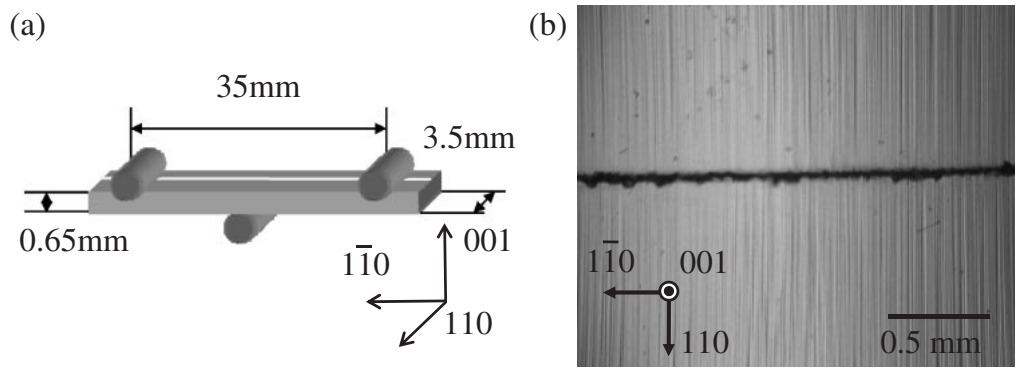

Fig. 1 (a) Schematic drawing of a three-pint bending sample. A scratch was introduced at the center of the specimen, (b) Optical micrograph around the scratch after deformation at 1023 K. Straight slip bans along [110] are observed.

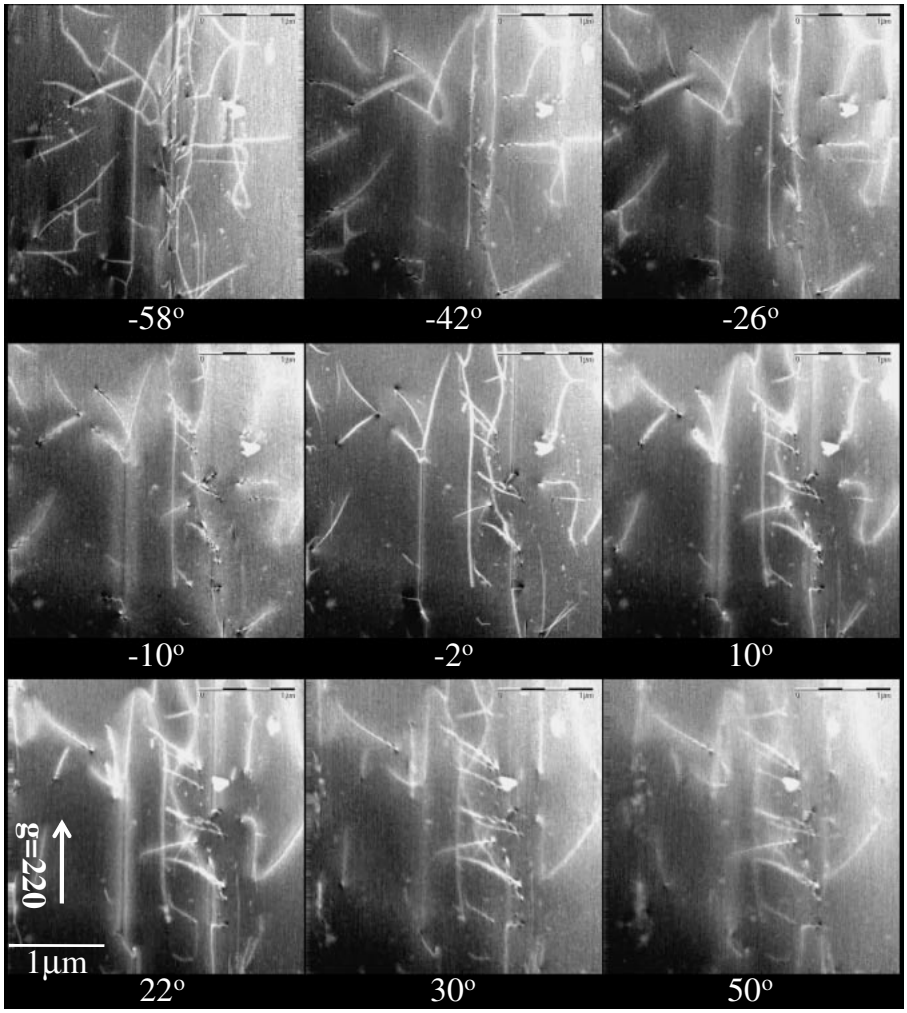

Fig. 2 Snap shots from a series of ADF-STEM images of dislocations. The specimen was tilted from -60° to 60°. The foil normal was [001]. The diffraction vector and tilting axis were kept nearly [220] during the equation of the images. Dislocations in some tilt angle indicate ambiguous due to the slight misorientation of the diffraction vector from 220.

3. Result and Discussions

Figure 2 shows snap shots of dislocations from a series of ADF-STEM images. The specimen was titled with an axis parallel to the [110] direction, so that the diffraction vector was nearly kept [220] during the acquisition of the images. The background of each image slightly contains diffraction contrasts, which reduces the quality of a reconstructed image. The diffraction contrast due to dislocations is distinguishable in all images acquired although some dislocation images are ambiguous due to the misorientation of the diffraction vector from [220]. The incident beam direction in the image taken with a title angle of -2° is almost parallel to [001] which is parallel to the foil normal. Some dislocation

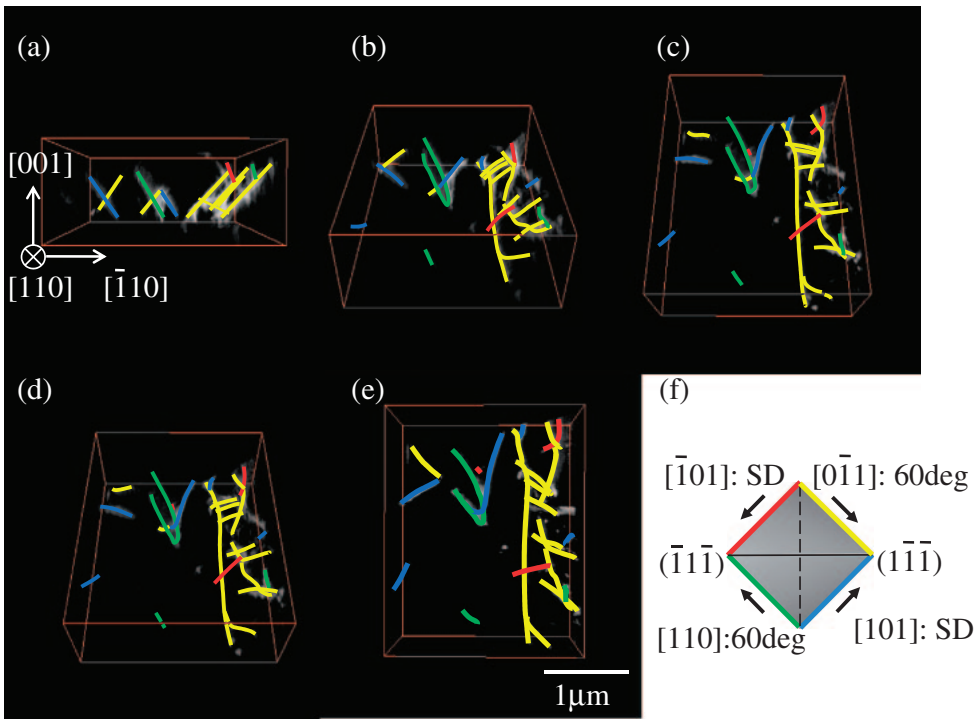

Fig. 3 Reconstructed dislocations by SIRT from a series of ADF-STEM image in Fig. 2. Each dislocation is colored in accordance with the color code of individual slip systems as shown on the Thompson tetrahedron in (f).

segments overlap each other when they are seen from this incident beam direction, so that the three-dimensional configuration of the dislocations is ambiguous. The Burgers vector of each dislocation was determined by the conventional invisibility criterion, $\boldsymbol{g} \cdot \boldsymbol{b} = 0$, in the parallel electron beam. All dislocations disappeared in the condition of $\boldsymbol{g}(hkl) = 040$, which indicates that the Burgers vector is either $a/2[\bar{1}01]$ or $a/2[101]$, where a is the lattice parameter. The slip planes of each dislocation were also determined by a reconstructed image obtained from Fig. 2.

Figure 3 exhibits a series of reconstructed dislocation images, where each dislocation is colored in accordance with the color code of individual slip systems as shown on the Thompson tetrahedron in Fig. 3(f). Figure 3(a) indicates a reconstructed image of dislocations seen from the [110] direction from which the observation was not actually possible. The dislocations are inclining to two different directions with respect to the surface, the (001) plane. The angles between the dislocation lines and the (001) plane were approximately 54°, which indicates that the dislocations are on the $(1\bar{1}\bar{1})$ or $(\bar{1}1\bar{1})$ planes, respectively. Most of the dislocations have the Burgers vector of $a/2[101]$ on the $(1\bar{1}\bar{1})$ plane while a few dislocations have the Burgers vector of $a/2[\bar{1}01]$ on the $(\bar{1}1\bar{1})$ plane. Although the Schmid factors of the two slip systems are the same under the tensile load along to $[\bar{1}10]$, one of the slip systems are preferentially activated.

The dislocation configuration is corresponds to the plastic deformation in plane stress condition in the tensile load as shown in Fig. 4, which is in good agreement with that the slip bands are formed parallel to the [110] direction. In addition, 60° dislocations are more frequently observed than pure screw dislocations. Pure screw dislocations would have diminished by gliding away to the surface while 60° dislocations were left in the sample since pure screw dislocations glide faster than 60° dislocations in silicon.[10)]

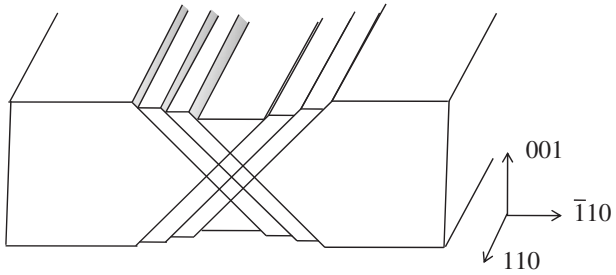

Fig. 4 Schematic drawing of the deformation step formed from the result of dislocation glide observed in Fig. 2.

4. Conclusion

Dislocations in slip bands in silicon single crystal were observed by ADF-STEM. The specimen holder was tilted from −60° to 60° with keeping the diffraction vector, $\boldsymbol{g}(hkl) = 220$. The reconstructed dislocation images indicate a three-dimensional configuration of the dislocations in the slip band. The application of electron tomography to the observation of dislocations has a high potential to analyze more complex dislocation configuration in three-dimension.

Acknowledgement

The authors appreciate that the work is partly supported by a Graint-in-Aid for Scientific Research (b) by The Ministry of Education, Culture, Sports, Science and Technology (KAKENHI#18360305).

REFERENCES

1) P. B. Hirsch, R. W. Horne and M. J. Whelan: Philos. Mag. **1** (1956) 677–684.
2) A. Klug and D. J. D. Rosier: Nature **212** (1966) 29–32.
3) M. Weyland: Top. Catal. **21** (2002) 175–183.
4) K. Kaneko, K. Inoke, K. Sato, K. Kitawaki, H. Higashida, I. Arslan and P. A. Midgley: Ultramicroscopy **108** (2008) 210–220.
5) K. Inoke, K. Kaneko, M. Weyl, P. A. Midgley, K. Higashida and Z. Horita: Acta Mater. **54** (2006) 2957–2963.
6) K. Kimura, S. Hata, S. Matsumura and T. Horiuchi: J. Electron Microsc. **54** (2005) 373–377.
7) J. S. Barnard, J. Sharp, J. R. Tong and P. A. Midgley: Science **313** (2006) 319.
8) J. S. Barnard, J. Sharp, J. R. Tong and P. A. Midgley: Philos. Mag. **86** (2006) 4901–4922.
9) R. Gordon, R. Bender and G. T. Herman: J. Theor. Biol. **29** (1970) 471–481.
10) M. Imai and K. Sumino: Philos. Mag. A **47** (1983) 599–621.